

Groundwater vulnerability mapping assessment of central West Bank catchments using PI method

Marwan Ghanem¹  · Waseem Ahmad² · Yacoub Keilan³ · Farah Sawaftah³

Received: 23 September 2016 / Accepted: 29 April 2017 / Published online: 9 May 2017
© Springer-Verlag Berlin Heidelberg 2017

Abstract A groundwater vulnerability assessment was carried out in order to understand and control the pollution sources affecting vulnerable regions in two adjacent catchments (Sarida and Natuf), located in the western middle part of the West Bank. The catchments were subjected to groundwater vulnerability mapping and assessment using the modified German State Geological Surveys (GLA method) method called Protective Cover and Infiltration Conditions method (PI method) via ArcGis 2014.2 software package in February of 2016. The results showed that the study area has high effectiveness of protective cover (*P*-factor), which was obtained by overlying top soil, bedrock, subsoil, and recharge layers. On the other hand, the dominant flow types, land usage, slopes, and topographical classification layers were overlaid to get the infiltration conditions (*I*-factor). The interaction between the two main factors was carried out in order to obtain the final spatially distributed π -factor values (vulnerability map), which was classified into four vulnerability classes. Statistically, about 4% of the overall area was of extreme vulnerability and concentrated along the sinking streams,

while 22% was of low vulnerability and existed outside the main watersheds, followed by high vulnerability with 26%. The largest proportion with 48% of the overall area was of moderate vulnerability to groundwater contamination.

Keywords Vulnerability mapping · PI method · West Bank · Groundwater

Introduction

Freshwater is a renewable resource, and it is more important to be sufficient for fulfilling people's needs. In semi-arid regions, the groundwater forms the largest amount of freshwater, while others such as permanent fresh rivers, lakes, and snowmelts are rare. The majority of the aquifers in the West Bank are karstic compared to others, due to the geological formations. It is well known that Middle East suffers from freshwater scarcity with karstic aquifer formations, which in turn are considered to be vulnerable to pollution sources and activities. Karstic aquifers, as a kind of groundwater reservoirs, are highly vulnerable to pollutants that dissolved in the infiltrated ground surface water or other surface water sources. The existence of direct pathways within unsaturated zones such as dolines and swallow holes contributes to consider the karstic aquifers as highly vulnerability to direct and indirect contaminations. Another minor reason was related to low soil depth that cannot play as remediation factor (COST 2003). Vulnerability is not only belonging to groundwater, but it related to anything or process that is exposed to high impact of any potential threat.

Generally, the non-karstic aquifers have less residence time for pollutants to reach groundwater; on the other hand, the fast and direct contamination is the most obvious

✉ Marwan Ghanem
mghanem@birzeit.edu

Waseem Ahmad
wasim.f.ahmed@gmail.com

Yacoub Keilan
keilani90@yahoo.com

Farah Sawaftah
sawaftaf@gmail.com

¹ Birzeit University, P.O. Box 14, Ramallah, Palestine

² Ministry of Health, Ramallah, Palestine

³ Ministry of Agriculture, Ramallah, Palestine

property of karsts (Kacaroglu 1999). Thus, there must be a real vigilance for such direct contamination particularly in strong rainfalls, storms, and hard runoffs that occur seasonally in order to assure groundwater quality within the aquifer (Polemio et al. 2009). Furthermore, there exists another reason for karstic aquifers creation related to human activities such as pollution increase and quarrying industries. Karst aquifers development could be adversely affected by these anthropogenic actions (Ford and William 2007; Polemio et al. 2009).

In general, the geographic information system (GIS) can be used for vulnerability mapping by spatial data handling, processing, analysis, and visualization (Burrough and McDonnell 1998). The overlay and index that was used in this study is GIS-based approach and considered as one of the traditional methods used to assess groundwater vulnerability to contamination; this approach helps in combining maps of the different inputs: geological, geomorphological, pedological, and hydrological data, which affect the transport of the pollutants from ground surface to groundwater (Witkowski et al. 2004). Moreover, it assigns an index values to those inputs, and the results of the data overlying process are spatially distributed vulnerability index. ArcGis 2014.2 is a GIS-based software package used this method to conduct the process and evaluate an area based on known conditions without the need for extensive specific pollution data.

Study area

The study area located at the western center of West Bank consisted of two catchments, which are Sarida and Natuf, where the geological formations start from the Jurassic to Quaternary periods, with the absence of any formations before Jurassic period (Abed and Wishahi 1999) (Fig. 1). It is located within the western aquifer basin, which is the largest groundwater aquifer in Palestine, where many seasonal and permanent springs spread through it. These springs emerge with an average discharge of 300–600 thousand cubic meters and used for domestic and agricultural activities. The only groundwater well is called Shibteen well related to Shibteen village and controlled by Israeli water authority.

The study area is bounded by Auja and Qilt catchments from the east and Qana catchment from the north, while Salman and Soreq catchment located south of the study area. The total length of the study area is about 36 km with width of 30 km and area of 1022 square kilometers. However, Natuf stream is considered as one of the two main streams in the area where the second is Sarida stream that originates from Salfit city and Ara'el Israeli colony, carrying and discharging their wastewater for several kilometers and affecting economic, social, and

public health aspects of the nearby communities, which are in turn about 80 communities distributing randomly in the area.

With 30 to 55 of rainy days distributing from early November to late April, the study area is classified as semiarid area with Mediterranean climate type where the summer season is long and dry, while winter is short and wet season (Ghanem 1999). With average rainfall of 540–740 mm/year, the mean rainfall decreases from East to West. January is considered as the coldest month of the year where the maximum temperature average is 30.1 °C and the minimum is 6.2 °C. August heats up to higher rates and considered as the highest temperature average with 39.1 °C, and the minimum temperature average is 19.5 °C (Khatib 2008).

Expressed by (RH %), the relative humidity increases by moving from east to west toward the coast at the level of the natural Palestine, and its average value ranges between 50% in the east regions to 70% in the west. In the study area where is almost located in the middle of this distance, the RH % yearly average is nearly 62% increases in winter up to 67% (Khatib 2008). Geologically, the western aquifer where the study area locates is considered as the Cenomanian–Turonian Limestone aquifer or “Judea Group” (Issar 2000). The aquifer is also classified as karst due to the function of dissolution process for permeable limestone system, which is in turn the major composing unit of the study area (Fig. 2).

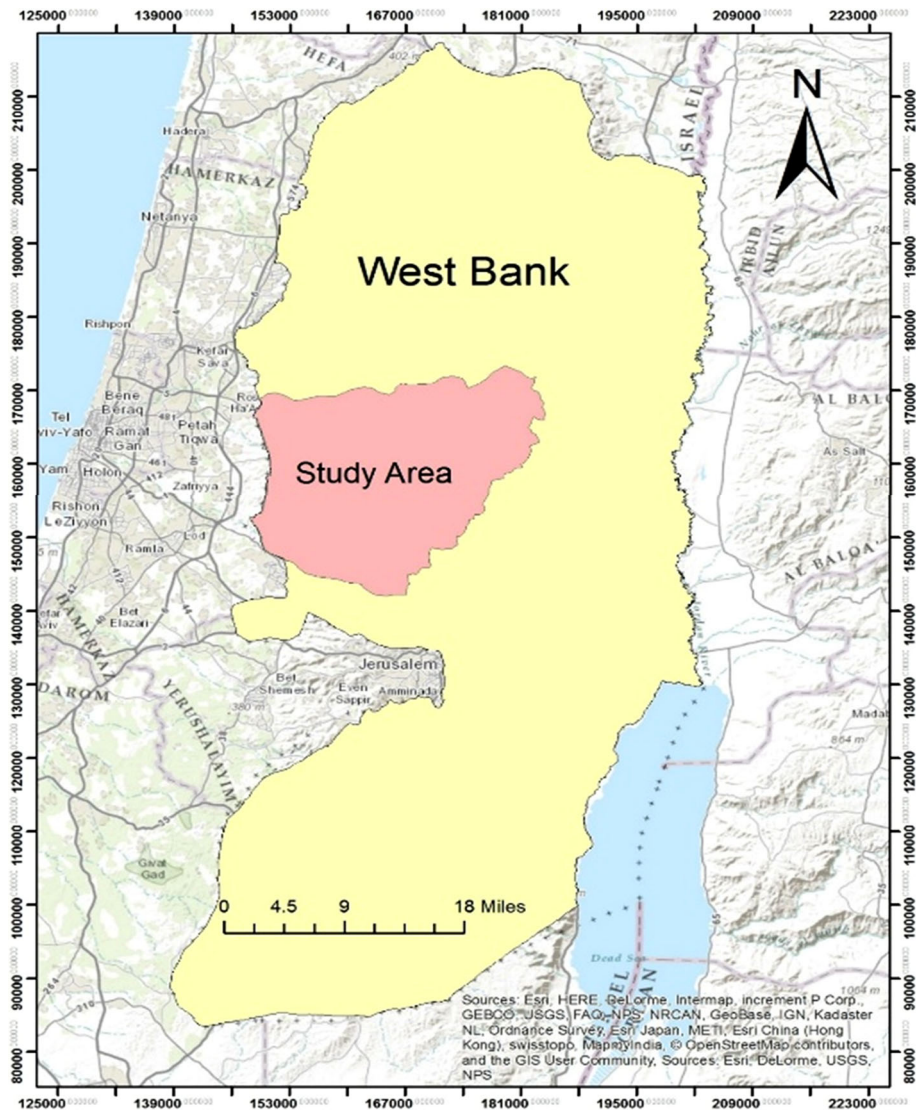
Cretaceous Group is divided into three major geological sections (SUSMAQ 2003):

1. Lower aquifer in the upper and lower Beit Kahil with 340 m thickness.
2. Mid. Cenomanian Aquiclude Yatta formation with average thickness is about 110 m.
3. Upper aquifer in the Turonian–Upper Cenomanian part with average thickness of 150 m.

For more specific, chalk, dolomite, limestone, and marl are the four major lithology types composing the aquifer formation with strata thickness ranging from 2 m up to 160 m in the eastern parts. Various fracturing levels are characterizing the strata where most of well-jointed karsts lie in the middle part of the study area, while faults and fractures are randomly distributed through the aquifer outcropping strata of the study area (Fig. 3).

It is obvious that the karstic formations in the middle of the study area are characterized with Albian formation age, while upper Cretaceous and upper Cenomanian formation ages are distributing in the west part of the aquifer. Regarding topography, the altitude of the study area varies from 34 m in the west increasing toward the east with up to 1004 m. However, the altitude difference between the both sides created various slope levels with majority slope of

Fig. 1 Study area location in the West Bank



less than 27%. As a result, many seasonal streams are formed and discharging toward the west.

Materials and methods

The DRASTIC method is not the proper method for karst aquifers vulnerability assessment (HWE 2009). Although the EPIK is the only method used until end of the twentieth century for karst aquifers, the GLA and PI methods showed more appropriate among other methods for such kind of formations (Zwahlen 2003) (Neukum et al. 2008). The modified PI method that was used for such purpose is GLA method, that was developed by Goldscheider (2003) in order to fix and fulfill the requirements of karst-related environments and take account of physical slowing down effect of the overlying

strata and could be used for all hydro-geological settings and formations (Margane 2003).

In this study, the PI method was used and developed within the scope of Programme of the European Commission on vulnerability and risk mapping for the protection of carbonate aquifers (COST Action 620) in the Department of Applied Geology (AGK) and published by Goldscheider et al. (2000b). This method and its modifications were used and applied in 12 karstic areas, such as:

- Hochifien-Gottesacker, Austro-German Alps (Goldscheider 2002).
- Winterstaude, Austrian Alps (Werz 2001).
- Mt. Cornacchia and Mt. della Meta, Latium, Italy (Coviello 2001).
- Mühltaquellen, Thuringia, Germany (Sauter et al. 2001).

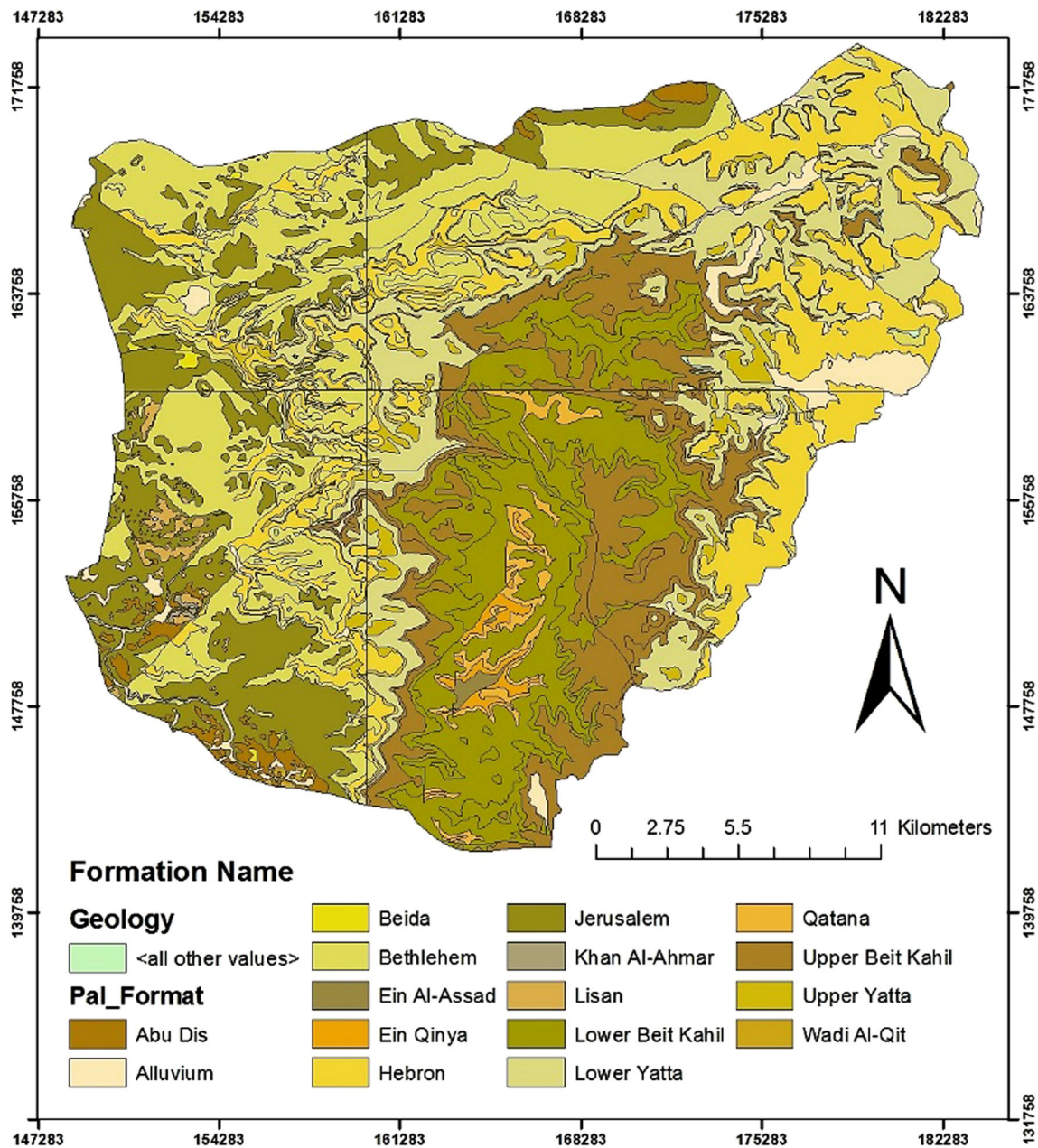


Fig. 2 Palestinian geological formations of Sarida and Natuf catchments

Actually, the PI method is based on origin–pathway–target conceptual model; this model is illustrated by the three components: the origin that refers to the contamination source at the ground surface, the pathway that is represented by the unsaturated zone with its soil and rock layers leading to the target component, which in turn refers to the top of groundwater table (Fig. 4).

The PI is an acronym that consists of the protective cover (*P*-factor) and the infiltration conditions (*I*-factor). *P*-factor expresses the protective action of the different rock layers between ground surface and groundwater surface including soil, subsoil, non-karstic rock, and unsaturated

karstic rock. On the other hand, the degree of penetration through protective layers to the groundwater is called *I*-factor, which is caused by the lateral surface flow and subsurface flow in the sinking streams and basins.

The result of overlying the two factors is the π -factor, which is spatially distributed and represented by vulnerability map and divided into five classes from 1 with the highest to 5 indicating the lowest vulnerability to contamination sources (Goldscheider 2002). Each factor is controlled by different input data with different scores that affect groundwater vulnerability levels. Thus, *P*-factor that has a large score after the summation is controlled by the

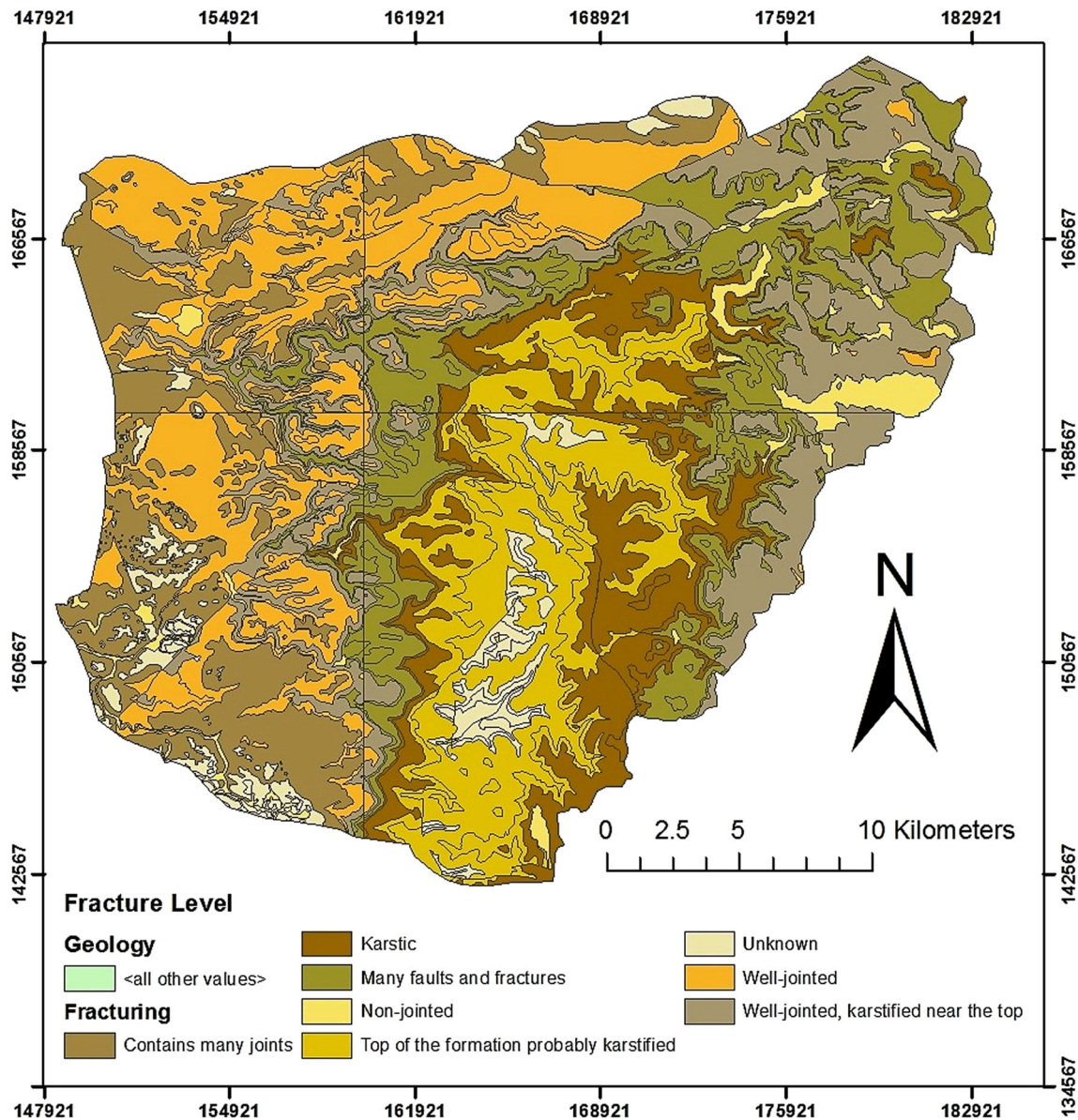


Fig. 3 Fracture level of the study area aquifer

following general formula of the total protective function (P_{TS}) (Goldscheider 2003):

$$P_{TS} = \left[T + \left(\sum_{i=1}^n B_i \cdot M_i + \sum_{l=1}^m S_l \cdot M_l \right) \right] \times R + A \quad (1)$$

where T top soil factor (T -factor), B bedrock score (Score- B), S subsoil factor (S -factor), R recharge factor (R -factor), M thickness of each layer, A artesian pressure.

The estimated field capacity (eFC) is the most soil property that could enhance the contamination mitigation by absorbing different amounts of liquid pollutants or rainfalls; these amounts are different according to soil types, particularly the soil structure (Table 1). The excess

amount of fluid continues its way downward the groundwater, crossing other rocky layers.

The bedrock score (B-score) is the result of multiplying the lithology factor (L -factor) which represents the lithology of the protective strata by the fracturing factor (F -factor), representing at how level stratum has fractures (Table 2).

Depending on the type of subsoil components, the S -factor received its values from each soil structure type (Table 3).

There is more than a method for intrinsic recharge determination, one of them is Goldscheider method that was used in this study. The important advantage of the

Fig. 4 Origin–pathway–target model (Krešić and Stevanović 2010)

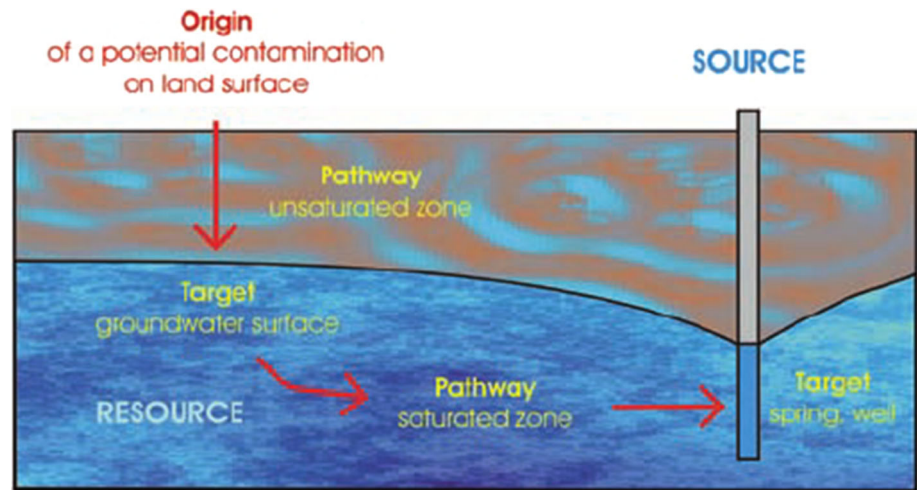


Table 1 Values of the factor of T (Goldscheider 2003)

eFC (mm) up to 1 m depth	T
>250	750
>100–250	500
>140–200	250
>90–140	125
>50–90	50
<50	0

method is to involve up to four factors affecting recharge ratio in each cell of the study area that ranges from 0 to 1 value. Land use in one of these factors, which was consisted into two classes: forest and other vegetation, each class has a certain impact on recharge ratio, this factor is associated with slope inclination factor, which also in turn was consisted into three classes: $<5^\circ$, 5° – 30° , $>30^\circ$ and significantly influencing the runoff ratio and therefore recharge ratio (Table 4).

On the other hand, the other two factors that are saturated hydraulic conductivity that varied from the value of 10^{-6} – 10^{-4} m/s and depth to low permeability layer had the main role to estimate the dominant flow process, which plays a significant effect for recharge ratio determination (Table 5).

The calculated recharge ratio as a result is a function of overlying the previously mentioned four factors based on

Table 2 L and F factor values for each type of lithology and fracturing (Goldscheider 2003)

Lithology	L	Fracturing	F
Claystone, slate, mart, siltstone	20	Non-jointed	25
Sandstone, quartzite, volcanic rock	15	Moderately joint, slightly karstified	1
Porous sandstone, volcanic rock	10	Moderately karstic	0.5
Conglomerate, limestone, dolomite	5	Strongly fractured	0.3

Table 3 Subsoil structure with attached S values (Goldscheider 2003)

Type of subsoil (grain size distribution)	S
Clay	500
Loamy clay, slightly silty clay	400
Silty clay, clayey silty loam	320

Table 4. The spatial distribution of rainfall in the study area would be needed to complete the process. A reclassification will also be needed in order to reclassify recharge values into new values called R -factor (Table 6).

The final value P_{TS} represents “the total protective function” and reclassified into five classes of the P -factor (Table 7).

The other main part of the PI method relates to the infiltration conditions (I -factor), which plays as significant protective cover by remediating a large part of the contaminants across soil and rocky layers, and is not prevalent in karst areas while completely bypassing fluids downwards, the groundwater and adversely affecting its quality due to the existence of sinking streams and swallow holes like in the case of karst areas of Sarida and Natuf catchments (Dyck and Peschike 1995).

In general, a three-step procedure is used in order to determine the final I -factor values: determination of the dominant flow process as previously mentioned,

Table 4 Recharged ratio caused by the dominant flow process, the vegetation, and the slope inclination (modified Goldscheider et al. 2000a)

Dominant flow process	<5° slope inclination		5°–30° slope inclination		>30° slope inclination	
	Forest	Other vegetation	Forest	Other vegetation	Forest	Other vegetation
Type A	1.0	1.0	1.0	1.0	1.0	0.8
Type B	1.0	1.0	0.8	0.6	0.6	0.4
Type C	1.0	1.0	0.6	0.4	0.4	0.2
Type D	0.8	0.6	0.6	0.4	0.4	0.2
Type E	1.0	0.8	0.6	0.4	0.4	0.2
Type F	0.8	0.6	0.4	0.2	0.2	0

Table 5 Determination of the predominant flow process as a function of the saturated hydraulic conductivity and the depth to low permeability layers (COST 2003)

Hydraulic conductivity (m/s)	1.E–04	Saturated surface flow	Very fast subsurface stormflow Fast subsurface stormflow	Infiltration and subsequent percolation	
	1.E–05	Hortonian surface flow rarely			
	1.E–06	Hortonian surface flow frequently			
		<30 cm	30–100 cm	>100 cm	
		Depth to low permeable layer (cm)			

Table 6 Reclassification of recharge values into new *R*-factor values (Goldscheider 2003)

Recharge (mm/year)	<i>R</i>	Recharge (mm/year)	<i>R</i>
0–100	1.75	>300–400	1.00
>100–200	1.50	>400	0.75
>200–300	1.25		

Table 7 Reclassification of Pts classes into *P*-factor new classes (Goldscheider 2003)

Score Pts	Effectiveness of protective cover	<i>P</i> -factor
0–10	Very low	1
>10–100	Low	2
>100–1000	Medium	3
>1000–10,000	High	4
>10,000	Very high	5

determination of the *I'* factor, and determination of the *I*-factor. Determination of *I'* factor values is essential input component for *I*-factor calculation, which is controlled by three variables, one of them is the land cover that is consisted into forest and other vegetation types. The second factor regarding the slope gradient percentage consisted into: <3.5%, 3.5–27% and >27%. Additionally, the dominant flow process types significantly affect the *I'* factor values. All of these variables interact with each other in

order to determine *I'* factor that is ranging from 0 as minimum value to 1 as maximum value (Table 8).

The values of *I*-factor range between 0.0 and 1.0, which could control the infiltration condition through the study area. This could be accomplished by the interaction between the *I'* factor values and the topographical classification of the study area, where each of the four zones has a certain impact on the resulting *I*-factor values and therefore the infiltration conditions (Table 9). In general, the lateral flow close to skinning streams is the most dangerous condition, while the flow leaving the karst system is the least dangerous (COST 2003).

The interaction according to formula (2) between the *P*-factor and *I*-factor is presenting the π -factor, which could be spatially distributed forming the vulnerability map, which in turn represents the degree of natural protection of the unsaturated zone and the intrinsic vulnerability across the map.

$$\pi = P \times I \tag{2}$$

The resulted π -factor is arranged in five classes where each class represents a vulnerability intensity with a certain color. The lowest degree of natural protection and sub-surface concentrated flow begins with red color, and 0–1 value range is considered to be the most vulnerable areas represented by sinking areas like sinking streams. The value of π -factor gradually increase 1 unit of value for each class with related color and ends with value of 4–5 value range with very low vulnerability degree (Table 10).

Table 8 Determination of I' factor values according to COST Action (2003)

Dominant flow process		Slope					
		<3.5%		3.5–27%		>27%	
		Forest	Others	Forest	Others	Forest	Others
Infiltration	Type A	1.0	1.0	1.0	1.0	1.0	0.8
Subsurface flow	Type B	1.0	1.0	0.8	0.6	0.6	0.4
	Type C	1.0	1.0	0.6	0.4	0.6	0.2
Surface flow	Type D	0.8	0.6	0.6	0.4	0.4	0.2
	Type E	1.0	0.8	0.6	0.4	0.4	0.2
	Type F	0.8	0.6	0.4	0.2	0.2	0.0

Table 9 The I' -factor values as a function of I' factor values and spatial zones (Goldscheider 2003)

Surface catchment map		I' factor					
		0.0	0.2	0.4	0.6	0.8	1.0
a	The 10-m buffer of the sinking streams	0.0	0.0	0.0	0.0	0.0	0.0
b	The 100-m buffer of the sinking streams	0.0	0.2	0.4	0.6	0.8	1.0
c	The surface watersheds of the sinking streams	0.2	0.4	0.6	0.8	1.0	1.0
d	The discharge of the flow inside the study area	1.0	1.0	1.0	1.0	1.0	1.0

Results and discussion

Vulnerability mapping was produced for the study area through developing a sequence of analyzing steps according to COST Action (2003).

Protective cover

One of these parts regards the efficiency of the protective strata referring to P -factor that could be obtained spatially by overlying the P -factor components, which in turn are illustrated by the P_{TS} general Eq. (1). Each component of P_{TS} as mentioned in the methodology is affecting the protective cover efficiency with different scores and different spatially distributed values.

Top soil effect

The eFC as an important property of soils is directly affecting the T -factor values, which in turn affect the

efficiency of the protective cover according to Eq. (1). About 89% of the study area is covered with Terra rossa, brown rendzinas, and pale rendzinas soil type, while about 8% is covered by brown rendzinas and pale rendzinas type, the other 3% is for grumusols and pale rendzinas soil type. All of the eFC of the mentioned soil types have values more than 250 mm/m and turned into T -factor values of 750 (Table 11).

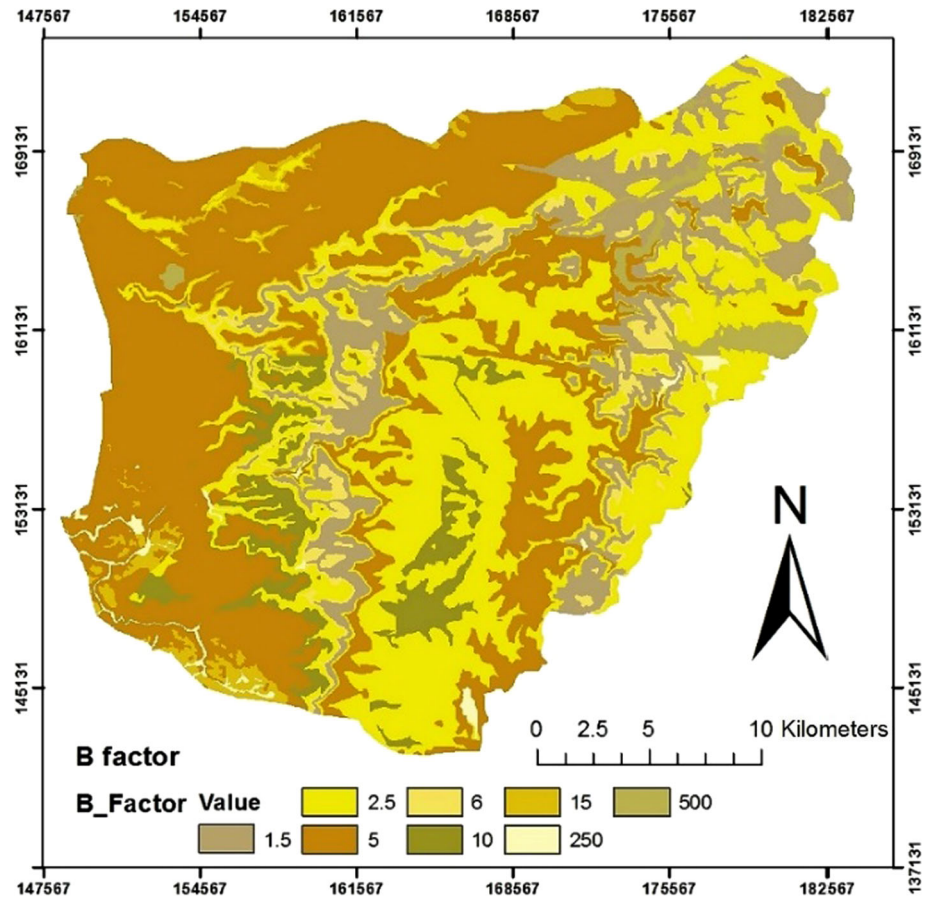
Bedrock effect

Depending on Table 2, each lithology type has a certain L -factor value; this factor plays a joint impact with the thickness of the strata in classifying the effects of the rocky protective cover. Three lithology types of dolomite, limestone, and marl are consisted of the majority of the study area formation. However, dolomite and limestone strata are representing about 61% of the overall area with L -factor value of 5 referring to low protective effect strata, and associated with F -factor of 0.3–0.5 which are also referring

Table 10 Legend for the vulnerability map, the P - and the I -map (Goldscheider 2003)

Vulnerability map vulnerability of groundwater			P -map protective function of overlying layers		I -map degree of bypassing	
	Description	π -factor	Description	P -factor	Description	I -factor
Red	Extreme	0–1	Very low	1	Very high	0.0–0.2
Orange	High	>1–2	Low	2	High	0.4
Yellow	Moderate	>2–3	Moderate	3	Moderate	0.6
Green	Low	>3–4	High	4	Low	0.8
Blue	Very low	>4–5	Very high	5	Very low	1.0

Fig. 6 Spatial distribution of B-score values depending on *L*- and *F*-factors



According to Goldscheider's (2003) predominant flow process classification method, the dominant flow process types were: fast subsurface storm flow coded by type B, saturated surface flow coded by type D, and Hortonian surface flow rarely coded by type E. These types were determined based on the available data of hydraulic conductivity and the depth to low permeable layer which was <40 cm (Table 5). The recharged ratio caused by the dominant flow process, the vegetation, and the slope inclination is illustrated in Table 4, and the actual recharged ratio results were spatially distributed through study area (Fig. 10).

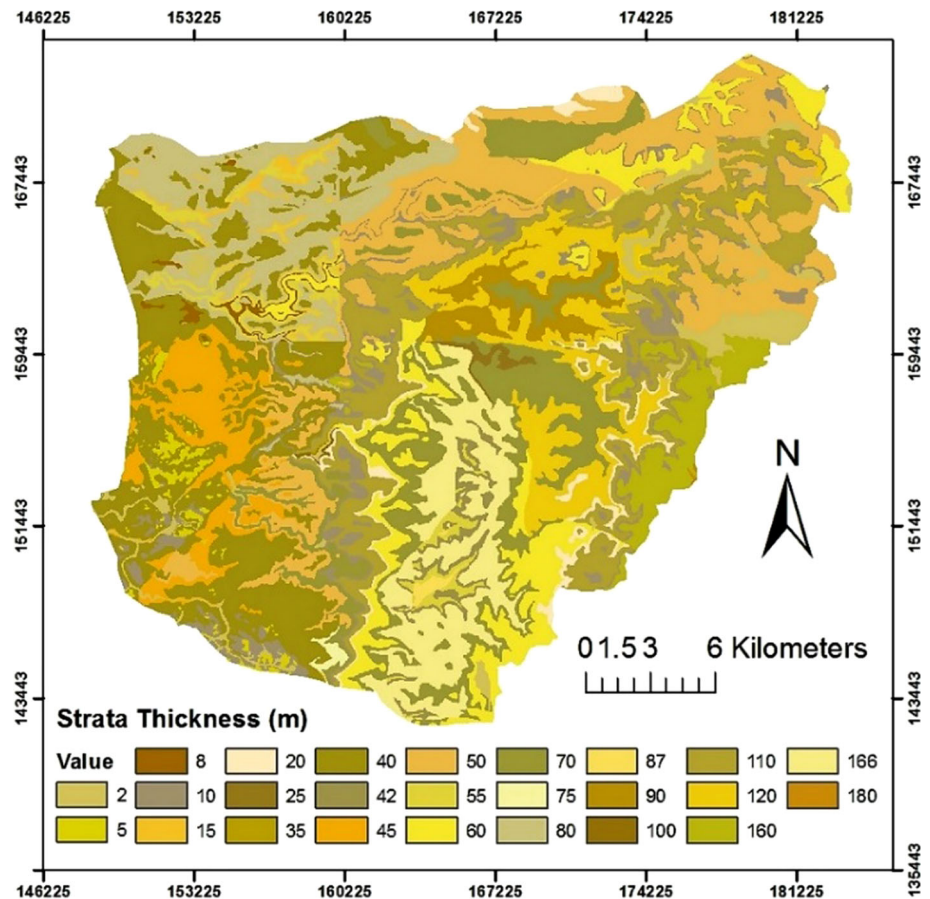
The less slope inclination has the high recharge ratio as shown in the northwestern parts of the study area, while the high ratio in the eastern part was caused by the Hortonian surface flow type, which obviously has a high impact and almost full recharge. The existence of forest stripe in the southwestern edge of the study area is responsible for such high recharge ratio (Fig. 10). The interaction between the actual rainfall values and the recharge ratio for the study area leads to the actual recharged values and spatially distributed (Fig. 11).

The recharge through the study area ranged from 67 mm in the western areas, increasing gradually toward

northern and eastern parts and showing higher recharged values up to 500 mm due to the higher rainfall amounts. However, total recharged mean for the study area is 197 mm. A reclassification for these values was accomplished in order to receive the *R*-factor values according to Table 6. The new values of *R*-factor included five classes where the value of 1.50 was the dominant, which in turn refers to 100–200 mm of recharge areas, while the least proportion was for a value of 1.00 referring to 300–400 mm recharge areas and distributed in the western areas of the map. The minimum value of 0.75 was mainly due to high slope, low soil conductivity, or low rainfall amounts, while the maximum value of 1.75 may be the function of low slope, high soil conductivity, and high rainfall amounts.

Depending on the geological formations of the study area, the artesian pressure (*A*-factor) in the aquifer was considered as additional score of $A = 1500$ and not modified in the PI method. The actual resulted values of score *P*_{ts} as a function of the general *P*_{ts} equation range from the value of 2305 as minimum value that refers to high effectiveness of protective cover, to the value of 5475 as maximum that also refers to high effectiveness of protective cover (Figs. 12, 13).

Fig. 7 Lithology thickness distribution through the study area



The *P*-factor values in the study were limited to value of 4 depending on the Pts class, which ranged from 1000 to 10,000 according to Table 7.

Infiltration conditions

According to Table 8, the interaction between the dominant flow process, gradient slope, and the land cover was used to determine the *I* factor values for each cell of the study area. It is obvious that high slopes in the middle of the study area with non-forest areas led to relatively lower infiltration conditions with ratio value of 0.2, while the peripheral area has higher value of 0.4 due to lower slope gradient with majority of the study area (Fig. 14).

The topographical classification of the study area had been spatially accomplished including four zones; each of them has a different impact on the *I* factor values according to Table 9 (Fig. 14).

The new resulted and modified values were called *I*-factor values, which could be spatially distributed to form *I*-map. Depending on the fact that *I*-factor is determining the degree to which the protective cover is bypassed by lateral surface and subsurface flow, it is clear that watershed areas with *I*-factor value of 0.6 and have the largest

proportion have moderate infiltration conditions. By turning into outside the watersheds, the values increase to 0.8, while the most dangerous infiltration conditions concentrated in the sinking streams and their buffer with values of 0, 0.2, respectively (Fig. 15).

Vulnerability map

By reference to Eq. (2), the *P*-factor relatively high value of 4 significantly affected the values of *I*-factor, resulting in the π -factor, which in turn refers to the natural protection degree of the unsaturated zone and the intrinsic vulnerability across the map, and could be spatially distributed to create groundwater vulnerability map or PI map (Fig. 16). This map could be classified into vulnerability levels to contamination with distinguishing colors based on Table 10. The groundwater vulnerability map describes how much we must wary about where we could set up risky and polluting facilities, especially industrial plants, extensive agricultural activities, landfills, and wastewater discharge locations.

Statistically, the least proportion among classes was the extreme vulnerability with red color representing about 4% of the overall area and concentrated in the sinking streams,

Fig. 8 Spatial distribution of BM score values through the study area

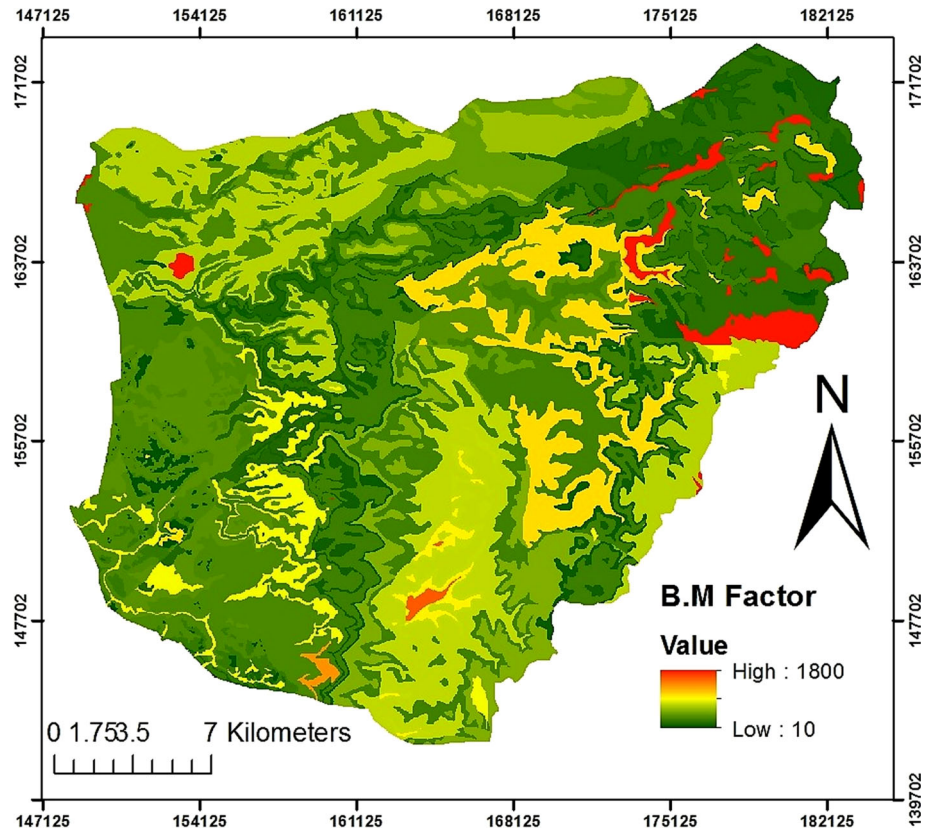


Fig. 9 Spatial distribution of S-factor values depending on the subsoil structure

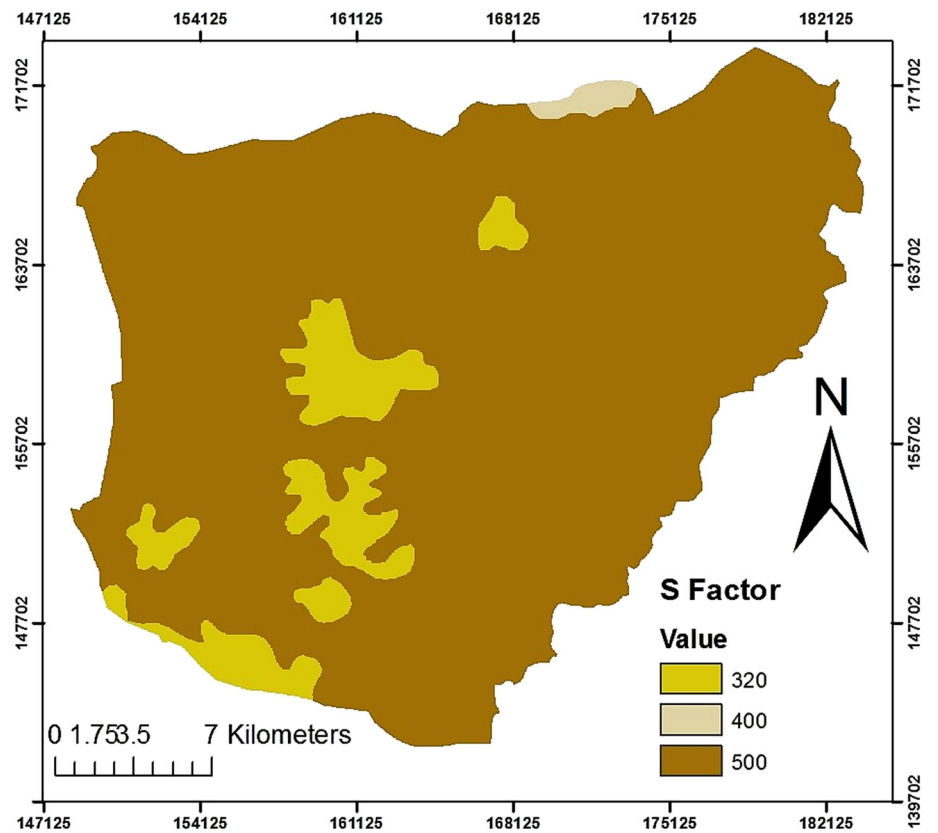


Fig. 10 Recharged ratio estimation in the study area based on modified Goldscheider method

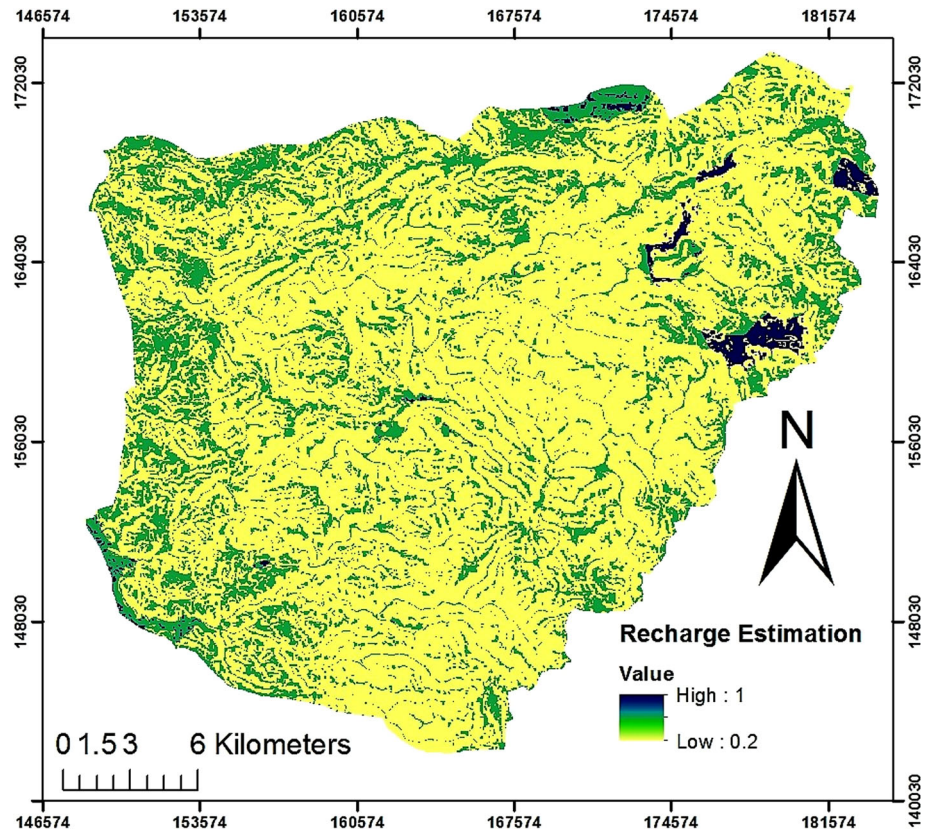


Fig. 11 Spatial distribution of the calculated recharge values across study area

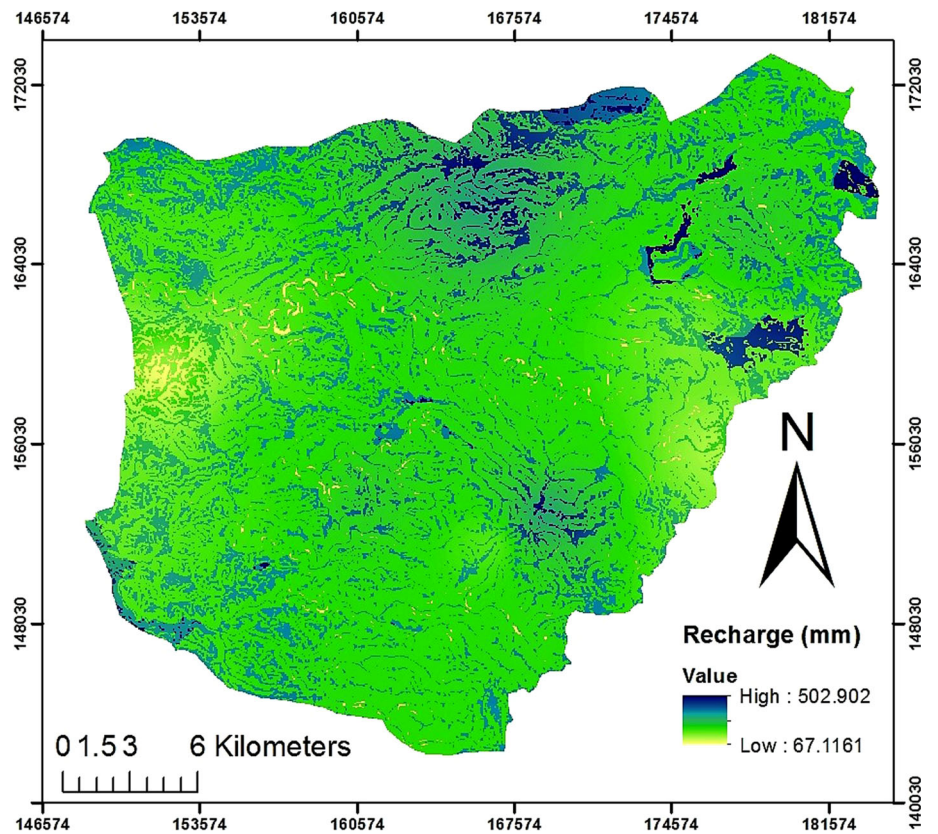


Fig. 12 Spatial distribution of the calculated Pts values as function of Pts general equation

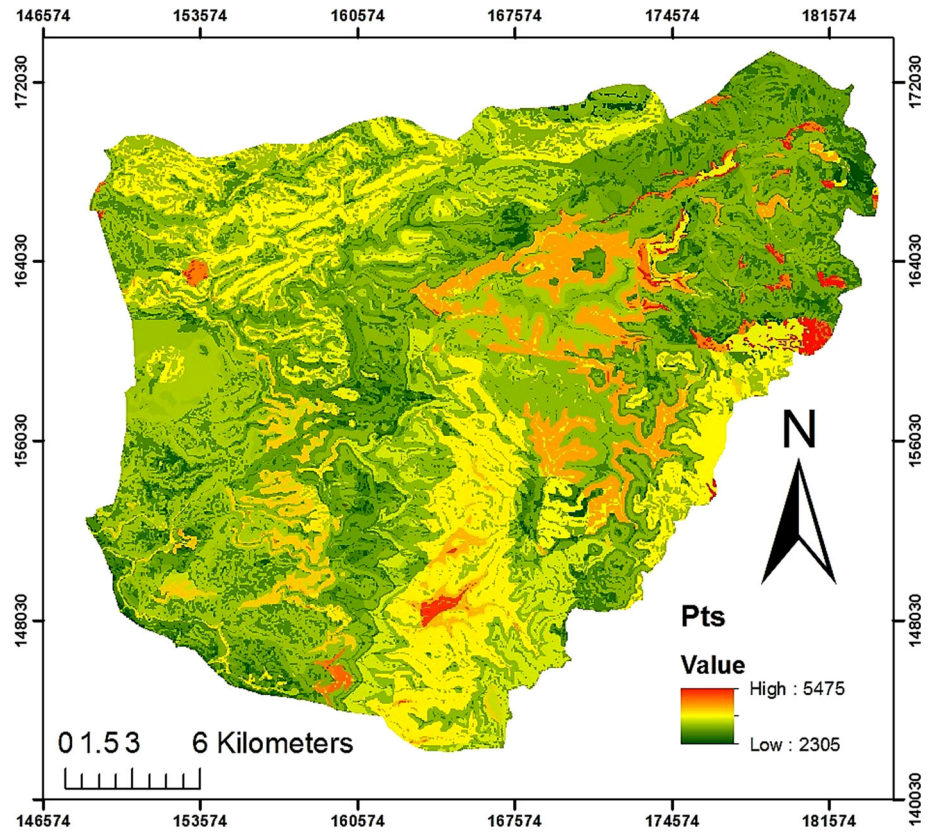


Fig. 13 Spatial distribution of the I' factor values as function of variable factors

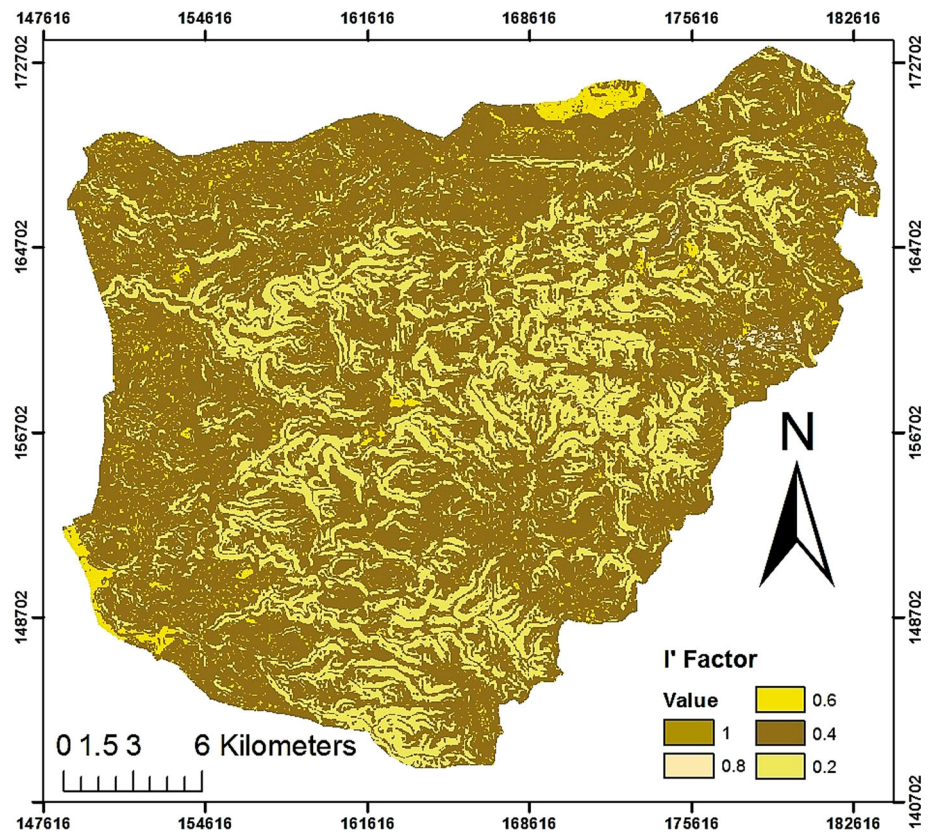


Fig. 14 Topographical classification of the study into four affecting zones

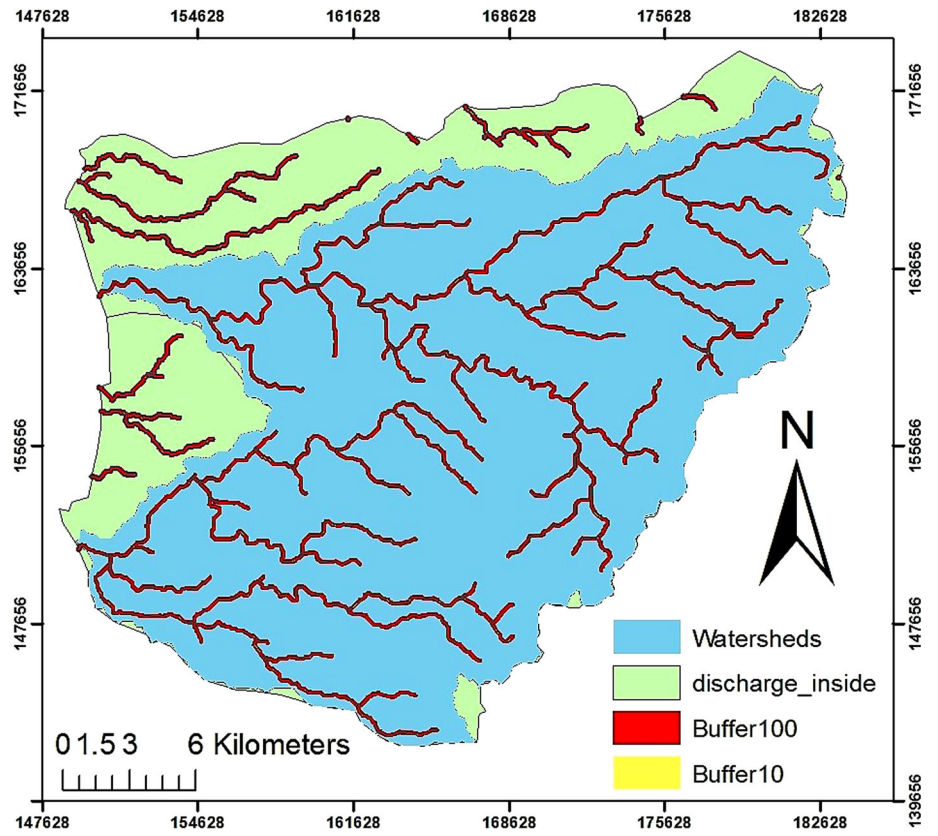
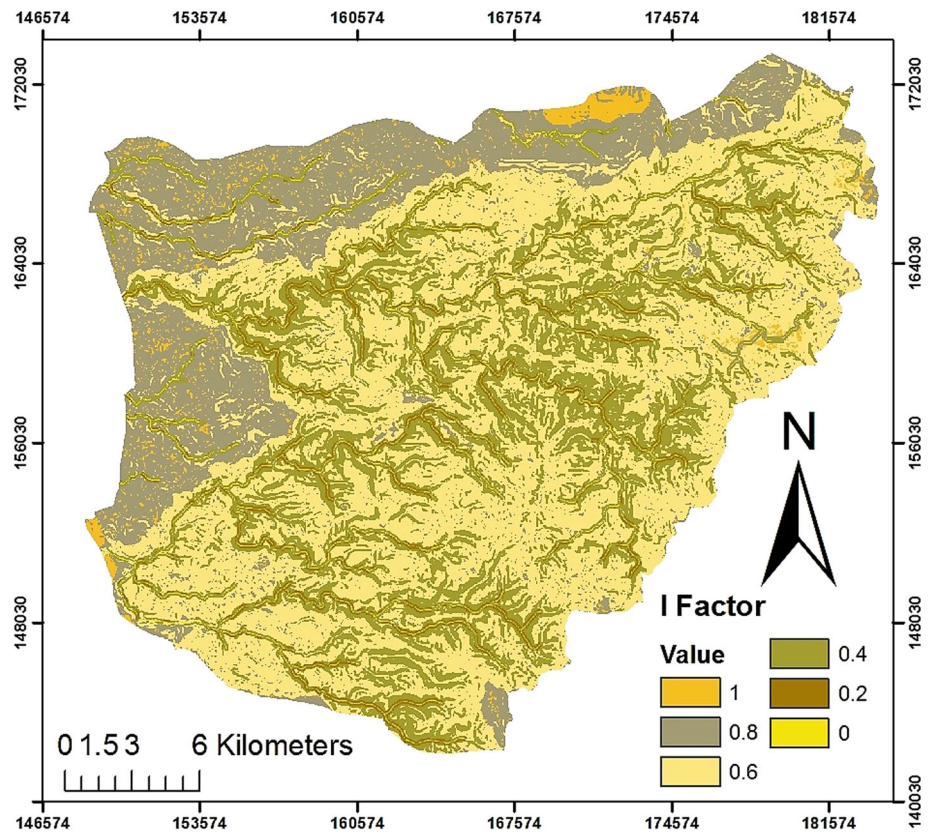


Fig. 15 Spatial distribution of the *I*-factor values as function of variable factors



the next larger proportion belonged to low vulnerability with green color and representing about 22% of overall area, the next class was for high vulnerability with orange color and representing about 26% of the overall area, and the final and larger proportion was for the moderate vulnerability degree with yellow color with about 48% of the overall area (Fig. 16).

There are various discipline methods regarding the validation assessment that required data, not provided in the groundwater vulnerability evaluation, for example biological, chemical properties, tracer method, and others (Daly et al. 2002). Based on this, data of water quality are available for many springs of the study area that acts as groundwater quality indicator. A new study was accomplished by Ahmad (2015) assessing biological and hydro-chemical quality of some springs water along Al-Matwi stream which flows raw wastewater originated from nearby localities. These springs acts as groundwater quality indicator and located within 100-m and 10-m buffers of the stream labeled as high and extreme vulnerable to contamination in the resulted vulnerability map (Table 12).

The results showed that all of these springs were contaminated with high counts of fecal coliforms and total coliforms as an action of the wastewater effect demonstrating the direct effect of the vulnerability level of the area to contamination (Table 13) (Ahmad 2015).

Additionally, vulnerability assessment was confirmed by the high values of NO_3 concentrations according to WHO limit for freshwater which is 10 mg/l (Ahmad 2015). There is also a chemical and microbial study for Natuf springs where most of them located out of the 100-m buffer and recorded as high quality for human uses; thus, these studies were consistent with the results of this groundwater vulnerability mapping study (Shalash 2006).

Conclusion

A relatively high field capacity with more than 205 mm/m was obvious and influenced the natural protective cover values positively using the COST Action 620 method. The combined effect of bedrock and subsoil factors showed high values, leading to high protective impact against the bypassed recharged water including dissolved contaminants, and therefore, less vulnerable depending on the fact that the less recharged amounts, the less potential contamination access and groundwater contamination. Several factors affected the recharge values as another important component, which ranged from 66 to 448 mm and distributed through the study area.

Additionally, there were three resulted dominant flow types affecting the natural protective cover which are: fast

Fig. 16 Spatial distribution of the reclassified π -factor values forming vulnerability

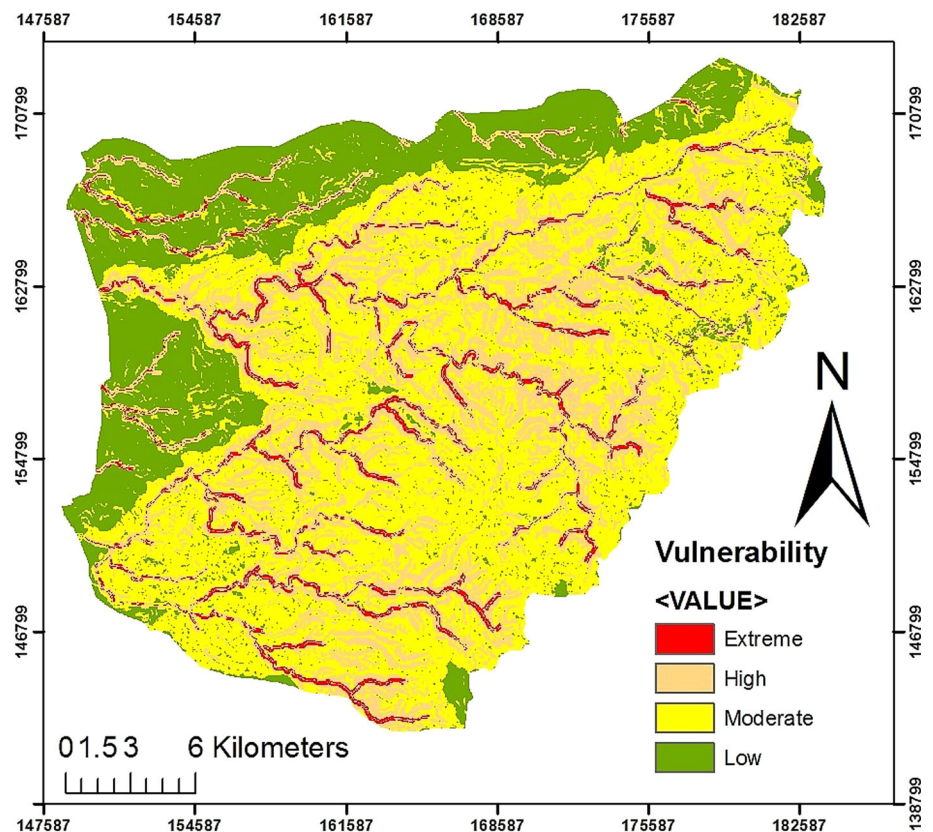


Table 12 Geographical coordinates (meters, Palestinian grids) of the springs along Sarida, Wadi

Station name	X	Y	Height
Al-Fawwar	159,727	163,643	278
Al-Yanbou	162,443	164,448	410
Al-Shalal	164,404	165,538	429
Al-Matwi	162,175	165,337	382
Al-Mizrab	164,448	164,314	343
Al-Adas	165,645	165,454	480

Table 13 Microbial and nitrate contents in springs along Sarida stream

Spring name	F.C (cfu/10 ml)	T.C (cfu/10 ml)	NO ₃ (mg/l)
Al-Fawwar	1000	10,600	46
Al-Yanbou	1300	23,000	20.9
Al-Shalal	12,000	120,000	46.3
Al-Matwi	500	13,000	41.7
Al-Mizrab	34,000	95,000	15.1
Al-Adas	1200	18,000	36.6

subsurface storm flow, Hortonian surface flow rarely, and saturated surface flow as the largest proportion. However, the relatively resulted high value of the *P*-factor was referred to the high natural protection cover of the unsaturated zone. On the other hand and based on the spatially distributed infiltration conditions factor values (*I*-factor), the low *I*-factor values were concentrated in the sinking streams buffers, referring to low meditating effect of the infiltration.

The resulted PI values that reclassified into four classes in the study case forming vulnerability map ranged from extreme vulnerable (0–1 value) to low vulnerable class (3–4 value) with the absence of very low vulnerability class (4–5 value), where most of vulnerable areas were concentrated along the sinking steams and their buffers, followed by the sinking steams watersheds that were obvious in the final vulnerability assessment map, while the lowest vulnerable areas belonged to outside of watersheds areas.

The statistical analysis of the vulnerability classification could be summarized with about 4% of the overall area, followed by low vulnerability with about 22% of overall area, the next class is for high vulnerability with about 26% of the overall area, and the final and larger proportion was for the moderate vulnerability degree representing about 48% of the overall area.

The applied examples of such vulnerability mapping assessment could help decision makers to controlling and authorizing the agricultural and industrial activities and

facilities particularly in the high vulnerable areas. It is recommended to carry out more evaluations and assessments of groundwater vulnerability at the local and regional levels.

References

Abed A, Wishahi S (1999) Geology of Palestine: the West Bank and Gaza Strip. Palestinian Hydrology Group, Jerusalem

Ahmad W (2015) The pollution effects of the wastewater flow on the water quality in Wadi Sarida catchment/West Bank, Master Thesis, Faculty of Graduate Studies, Birzeit University, Palestine

Burrough P, McDonnell R (1998) Principles of geographical information systems. Oxford University Press, Oxford

COST (2003) Action 620—Vulnerability and risk mapping for the protection of carbonate (karst) aquifers, European Commission, Directorate-General for Research, Report EUR 20912, Luxemburg

Coviello M (2001) Vulnerabilita' del Bacino di Alimentazione delle Sorgenti di Posta Fibreno (FR). Master thesis, Università degli Studi di Roma, D.I.T.S., Roma (**unpublished**)

Daly D, Dassargues A, Drew D, Dunne S, Goldscheider N, Neale S, Popescu I, Zwahlen F (2002) Main concepts of the “European approach” to karst-groundwater-vulnerability assessment and mapping. *Hydrogeol J* 10(2):340–345

Dyck S, Peschke G (1995) Grundlagen der Hydrologie. Verlag für Bauwesen, Berlin

Ford D, Williams P (2007) Karst hydrogeology and geomorphology. Wiley, Chichester

Ghanem M (1999) Hydrology and hydrochemistry of the faria drainage basin/West Bank, Ph.D. Thesis, Technische Universität Bergakademie Freiberg

Goldscheider N (2002) Hydrogeology and vulnerability of karst systems—examples from the Northern Alps and Swabian Alb. *Schr. Angew. Geol. Karlsruhe*, vol 68. www.ubka.uni-karlsruhe.de/vvv/2002/bio-geo/3/3.pdf

Goldscheider N (2003) The PI method. In: Zwahlen F (ed) Vulnerability and risk mapping for the protection of carbonate (karst) aquifers, Final Report (COST action 620). European Commission, Directorate-General XII Science, Research and Development, Brussels, pp 144–155

Goldscheider N, Klute M, Sturm S, Hötzl H (2000a) The PI method—a GIS-based approach to mapping groundwater vulnerability with special consideration of karst aquifers. *Z Angew Geol* 46(3):157–166

Goldscheider N, Klute M, Sturm S, Hötzl H (2000b) The PI method—a GIS-based approach to mapping groundwater vulnerability with special consideration of karst aquifers. *Z Angew Geol* 46(3):157–166

HWE—House of Water and Environment (2009) Assessment of groundwater vulnerability for ramallah wastewater treatment plant. House of Water and Environment, Ramallah, Palestine

Issar A (2000) Water—the past is the key to the future, the water resources of Israel, past present and future, a comprehensive outline. 29 July 2005. <http://www.mideastwe.org/water3.html>

Kacaroglu F (1999) Review of groundwater pollution and protection in karst areas, Kluwer Academic Publishers. *Water Air Soil Pollut* 113:337–356

Khatib R (2008) The impact of Israeli settlements on ruban expansion of residential agglomerations in Salfit Governorate. An-Najah National University, Unpublished Master Thesis

Krešić N, Stevanović Z (2010) Groundwater hydrology of springs, 1st edition: engineering, theory, management and sustainability.

- Butterworth-Heinemann publisher, Elsevier. ISBN: 9780080949451
- Margane A (2003) Management, protection and sustainable use of groundwater and soil resources in the Arab region. Guideline for Groundwater vulnerability mapping and risk assessment for the susceptibility of groundwater resources to contamination, vol 4, Damascus
- Neukum C, Hötzl H, Himmelsbach T (2008) Validation of vulnerability mapping methods by field investigations and numerical modelling. *Hydrogeol J* 16(4):641–658
- Polemio M, Dragone V, Limoni P (2009) Monitoring and methods to analyse the groundwater quality degradation risk in coastal karstic aquifers (Apulia, Southern Italy). *Environ Geol* 58(2):299–312
- Sauter M, Herch A, Jungstand P, Siebert C, Koch C (2001) Kartierung der Grundwasserver-schmutzungsempfindlichkeit im Muschelkalkaquifer am Beispiel des Einzugsgebietes der Mühlthalquellen bei Jena, Thüringen. Final report (**unpublished**)
- Shalash I (2006) Hydrochemistry of the Natuf drainage basin Ramallah/West Bank, Master Thesis, Faculty of Graduate Studies, Birzeit University
- SUSMAQ (2003) Field Measurement campaign for Wadi Natuf recharge estimation: background, design and workshop—NAT#48V0.3. Palestinian Water Authority, Palestine
- Werz H (2001) Kartierung der Geologie, Hydrogeologie und Vulnerabilität im alpinen Karst als Grundlage eines Konzeptes zum Trinkwasserschutz für die Gemeinde Bezau (Bregenzer Wald, Österreich). Master thesis Univ. Karlsruhe, Karlsruhe (**unpublished**)
- Witkowski A, Kowalczyk A, Vrba J (2004) Groundwater vulnerability assessment and mapping: selected papers from the groundwater assessment and mapping international conference - IAH - Selected Papers on Hydrogeology) - Kindle Edition. Amazon Publisher, Ustron. ISBN-13: 978-0415445610
- Zwahlen F (2003) Vulnerability and risk mapping for the protection of carbonate (karst) aquifers, Final Report (COST action 620). European Commission, Directorate-General XII Science, Research and Development, Brussels